Available online at www.sciencedirect.com
SCIENCE DIRECT
Materials Research Bulletin 41 (2006) 1476–1486
Materials Research Bulletin
www.elsevier.com/locate/matresbu

Polyol mediated synthesis of tungsten trioxide and Ti doped tungsten trioxide
Part 1: Synthesis and characterisation of the precursor material

P. Porkodi, V. Yegnaraman, D. Jeyakumar *

Electrodics and Electrocatalysis Division, Central Electrochemical Research Institute, Karaikudi 630006, India

Received 25 July 2005; received in revised form 13 January 2006; accepted 23 January 2006
Available online 21 February 2006

Abstract

Polyol mediated synthesis for the preparation of tungsten trioxide and titanium doped tungsten trioxide has been reported. The reaction was carried out using chlorides of tungsten and titanium in diethylene glycol medium and water as the reagent for hydrolysis at 190 °C. Formation of a blue coloured dimensionally stable suspension of the precursor materials was observed during the course of the reaction. The particle sizes of the precursor materials were observed to be around 100 nm. The precursor materials were annealed to give tungsten trioxide and titanium doped tungsten trioxide. The precursor materials were characterised using TGA/DTA, FT-IR, optical spectra, SEM, TEM and powder XRD methods. It was observed that the doping of titanium could be effected at least up to 10% of Ti in WO_3. The TGA/DTA studies indicated that $WO_{3-x}{\cdot}H_2O$ is the dominant material that formed during the polyol mediated synthesis. The XRD data of the annealed samples revealed that the crystalline phase could be manipulated by varying the extent of titanium doping in the tungsten trioxide matrix.

Keywords: A. Oxides; A. Semiconductors; C. Infrared spectroscopy; C. Thermogravimetric analysis; C. X-ray diffraction

1. Introduction

Tungsten trioxide has received much attention recently due to its potential in many technological applications, viz., electrochromic devices [1–4], photochromic devices [5,6] and gas sensors [7–12]. WCl_6 is a reactive molecule and readily hydrolysed in the presence of water to form tungstic acid, which can be annealed at the desired temperature to yield WO_3. However, the morphology and particle size of the product cannot be controlled. Hence, several synthetic routes have been adopted for the preparation of WO_3 that include aqueous alcoholic synthesis [9], pyrolysis [10], sol–co-precipitation [7,11], sol–gel method [9,12], emulsion method and ion exchange method [13].

In aqueous alcoholic synthesis, a mixture of WCl_6 and 2,4-pentadione in absolute ethanol was sonicated at 40 °C for 2 h and allowed to stand at room temperature for 2 h. The precipitate formed was separated and annealed at 850 °C

* Corresponding author. Tel.: +91 4565 226204.
E-mail address: djkr@rediffmail.com (D. Jeyakumar).

0025-5408/$ – see front matter © 2006 Published by Elsevier Ltd.
doi:10.1016/j.materresbull.2006.01.030

for 1 h to yield the yellow WO_3. A similar procedure has been adopted in the sol–gel process, wherein WCl_6 is dissolved in ethanol to which 2,4-pentadione and water were added. The mixture was allowed to stand for 14 h to get the sol. After evaporating the solvent, the powder is crushed and annealed at 850 °C for 1 h to get WO_3. In yet another variation of the synthetic procedure, WCl_6 is mixed with a surfactant and ammonium hydroxide and the resultant precipitate was separated and processed further to get WO_3. In all these cases, though the reaction conditions are not cumbersome, it is often essential to maintain the reaction conditions meticulously, especially if we desire to get nanosized particles of WO_3. Alternatively, ammonium paratungstate was pyrolysed at 500 °C for 5 h and the resultant material was crushed in a planetary ball mill for 30 min to get WO_3 powder in micrometer range. In emulsion-based synthesis, Na_2WO_4 was passed through the cation exchange resin and the H_2WO_4 exiting from resin was dripped into a solution containing either oxalate and acetate ion exchange ligand or water in oil-based emulsion. The solution stirred for three days and further processed to get WO_3. In addition to the above there are other preparative routes wherein peroxotungstate was used as precursor [3,14,15] for the preparation of WO_3. Komornicki et al. [15] have reported that 1.15 mol% of Ti could be doped in WO_3 by this route. However, they have observed that rutile phase appeared separately at higher Ti concentration.

Depero et al. has carried out the XRD simulation studies of WO_3 and predicted that by suitably introducing static disorder, either by oxygen deficiency in the matrix or by substituting the W by metal ions with lower oxidation states, different crystalline phases of WO_3 can be obtained. W(VI) and Ti(IV) have almost the same size (ionic radii 0.074 nm) and are known to occupy the same site. An attempt has been made to vary the level of doping of Ti in WO_3 matrix and study the nature of the phase formation. For this purpose, it is felt that the preparative condition should ensure atomic level mixing of Ti(IV) with W(VI) in solution.

Polyol mediated synthesis of materials is an attractive route, as the reaction conditions are simple and elegant that yields nano sized particles in the form of dimensionally stable colloidal suspensions. This method employs high boiling polyols, such as diethylene glycol, glycerol, glycol, etc., as the reaction medium [16–18] for the preparation of oxide materials. Suitable reactants from homogenous solution (metal acetates/chlorides/alkoxides) are hydrolysed at elevated temperature (ca. 190 °C) resulting in the formation of nano metal oxides/precursors as suspension in polyol. It may be noted that the colloidally stable suspension can be used for coating the material onto desired substrates. More importantly the reaction is carried out in homogenous solution which ensure atomic level mixing of reagents is ensured and more apt to prepare Ti doped WO_3 matrix.

Over and above, doping of Ti in WO_3 matrix resulted in the increased sensitivity of NO_X sensors. There is no systematic study on the preparation of Ti doping in WO_3 matrix and evaluating the material characteristics for gas sensing. Hence, an attempt has been made to utilise the versatility of polyol-mediated synthetic method for the preparation of nano sized WO_3 and Ti doped WO_3.

2. Experimental

2.1. Synthesis of WO_3 and Ti doped WO_3

WCl_6 (14.4 g) was added to 200 ml of diethylene glycol (DEG) and the solution was heated in an oil bath at 80 °C to give a pale yellow coloured solution and to this solution 40 ml of distilled water was added, the temperature was raised to 190 °C and refluxed for 3 h. The yellow coloured solution immediately turned into pale green colour and gradually changed to a deep blue coloured suspension. The precipitate was separated by centrifuging, boiled with ethanol and washed thoroughly to remove DEG. The precipitate thus obtained was dried to form a fine powder by evaporating in a Roto-evaporator system. The yield of the material was around 7.1 g. The blue coloured precursor was used for further studies.

A similar preparative procedure was adopted for the preparation of titanium doped WO_3 precursors, wherein required amount of $TiCl_4$ in propanol was added to the WCl_6 solution. The level of doping was varied by using 1% or 10% (of $TiCl_4$ solution) by weight of WCl_6. Atomic level mixing is ensured as the reaction has been carried out in homogeneous solution and hence, uniform doping of Ti in WO_3 matrix is expected. For all the compositions like in the case of WCl_6 alone, blue coloured precursor materials were obtained. The materials were centrifuged, boiled with ethanol and washed repeatedly with ethanol to give the precursor materials. The blue precursor formed is annealed at various temperatures, ca., 150 °C, 300 °C, 400 °C, 500 °C, 600 °C, 700 °C and 800 °C.

2.2. Characterization

The FT-IR spectra of the samples (precursor and the annealed materials) were recorded in KBr pellet using Nexus FT-IR spectrometer 670 Model with DIGS detector. The optical spectra for the precursor samples were recorded using Cary 500 scan UV–vis–NIR spectrophotometer. Optically clear glass plates were used as substrates for the measurement of optical absorption spectra. The precursors/annealed samples at 700 °C were dispersed in absolute ethanol and sonicated well. The solution was coated onto the glass substrate by spin coating (Milman spin coater). The spin coated thin films were used for the absorption measurements. The XRD powder pattern of the precursor as well as the samples annealed at various temperatures were measured using Cu Kα radiation (Philips PANalytical Model 'X' Pert PRO). TGA/DTA studies were carried out using (PL-STA 1000/1500) at a heating rate of 20 °C/min. The surface morphology of the particles was studied using scanning electron microscope (JEOL JSM CF-35) and Transmission Electron Microscope (CM200 SuperPower STEM). The cyclic voltammetric studies were carried out using a Wenking Potentioscan Model POS 88 in conjunction with a Rikadenki x, y-t recorder. A three-electrode assembly used in this study comprised a precursor coated Pt electrode (5 mm × 5 mm), a platinum wire counter electrode and Hg/Hg_2SO_4 (1.0 M H_2SO_4) reference electrode.

3. Results and discussion

3.1. Preparation of precursor material

WCl_6 gave a yellow coloured solution in diethyleneglycol, which turned into a pale green colour solution. On hydrolysis at 190 °C in the presence of water gave a deep blue coloured colloidal solution. If the hydrolysis of WCl_6 alone is the anticipated reaction one may expect to get a yellow coloured $WO_3{\cdot}H_2O$ as the product. However, this is not the case when an alcohol was used as the reaction medium. This is due to the fact that W(VI) is a moderate oxidising agent. Polyol has been reported to act as a reducing agent for noble metal ions [16]. Hence, W(VI) has been partly reduced to W(V) in polyol to give a deep blue coloured non-stoichiometric precursor. It is established that the polyol-mediated synthesis generally yields nanosized particles and in the present case a colloidally stable blue coloured suspension. The colloidal solution was centrifuged and washed thoroughly with ethanol to yield the precursor material. WO_3 and the Ti doped WO_3 materials were all deeply blue coloured immediately after isolation and were used for the characterisation of the materials. It may be interesting to note that the precursor of tungsten trioxide remained blue in colour on prolonged storage, wherein the 1% titanium doped material gradually changed to green coloured sample and the 10% titanium doped sample turned into yellow coloured sample.

The precursor materials were annealed at high temperature to give light yellow to bright yellow coloured tungsten oxide materials. This change in the colour may be due to the fact that the non-stoichiometric tungsten trioxide has been oxidised to WO_3 in the presence of air at high temperature. The same process would have been facilitated if titanium was present in the matrix of the precursor.

3.2. TGA/DTA analysis

Fig. 1a depicts the TGA/DTA of the blue precursor obtained by the hydrolysis of WCl_6 in polyol medium. It can be seen from the figure that the precursor undergoes thermal decomposition by a number of exothermic processes with a weight loss of 6.57%. This value corresponds to $WO_3{\cdot}H_2O$, wherein the loss of 7.2% is expected. Similar observations have been made by Gotic et al. [21], wherein they have prepared $WO_3{\cdot}H_2O$ by ion exchange method from Na_2WO_4 and the TG studies showed the weight loss of 6.6%. The first exothermic process was very broad around 150 °C under which the weight loss was maximum. The second exothermic peak was also slightly broad (at 261 °C) with a minimum weight loss and the third process took place at about 489 °C after which there was an increase in the weight of the sample due to the oxidation of WO_{3-x} to WO_3. These observations suggest that the precursor formed may be $WO_{3-x}{\cdot}H_2O$. The TGA/DTA of the Ti doped precursors are presented in Fig. 1b and c. In both the cases it has been observed that the nature of the processes were exothermic as in the case of WO_3 precursor. The first peak appears around 150 °C as a broad one and the second exothermic peak around 295 °C. The third exothermic process observed in the case of WO_3 precursor was not present, however, the trend of increase in the weight after 600 °C was observed. In addition, the weight loss was increased from 6.56% to 9.7% and 13.3% for 1% and 10% Ti doped WO_3 precursors,

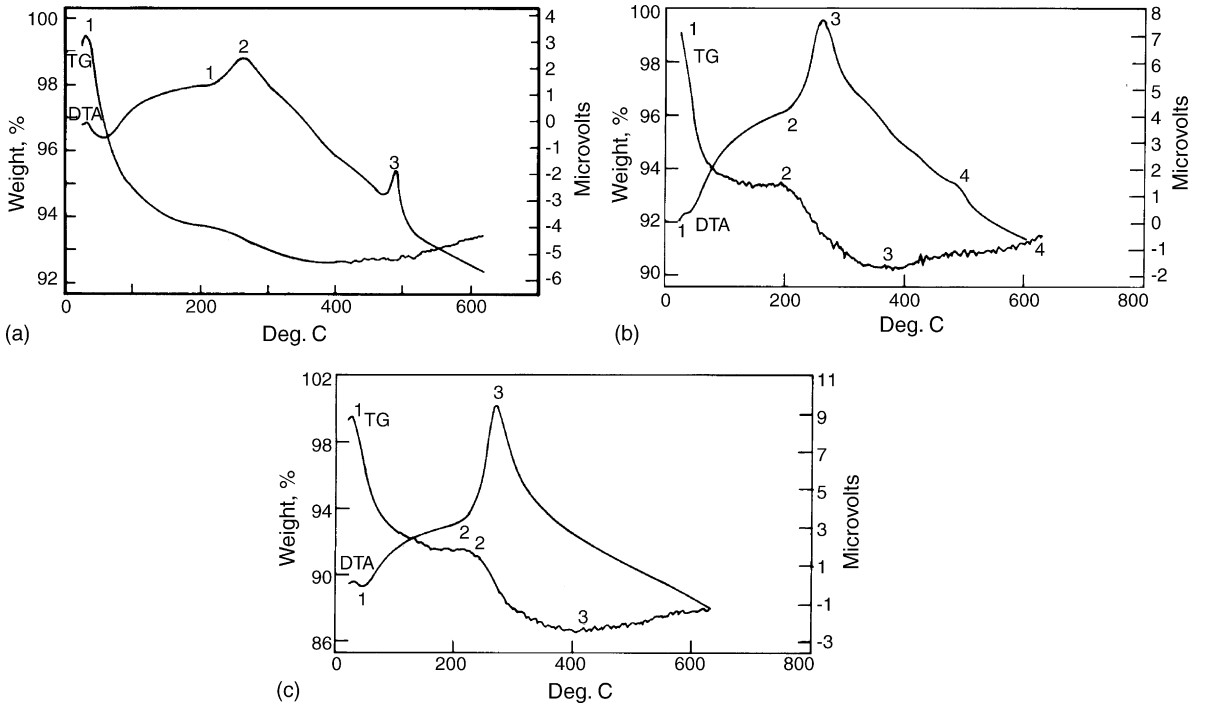

Fig. 1. TGA/DTA profiles of: (a) WO_3-precursor, (b) WO_3:1% Ti-precursor, (c) WO_3:10% Ti-precursor.

respectively. This is due to the formation of $Ti(OH)_4$ in the precursor. To confirm this $TiCl_4$ was hydrolysed in polyol medium by water wherein a white coloured material was obtained. The material was isolated and washed thoroughly with alcohol to remove the diethylene glycol and then dried. The material thus obtained was subjected to TGA study and 30% weight loss observed.

3.3. FT-IR spectra

Fig. 2 shows the FT-IR spectrum of WO_3 precursor recorded in the region 400–4000 cm^{-1}. The peaks of the precursor formed resemble to that of the tungstic acid. The very broad band from 1000 cm^{-1} to 500 cm^{-1} in WO_3 precursor corresponds to the W–O vibrational mode. The peak at 806 cm^{-1} of the precursor material is O–W–O

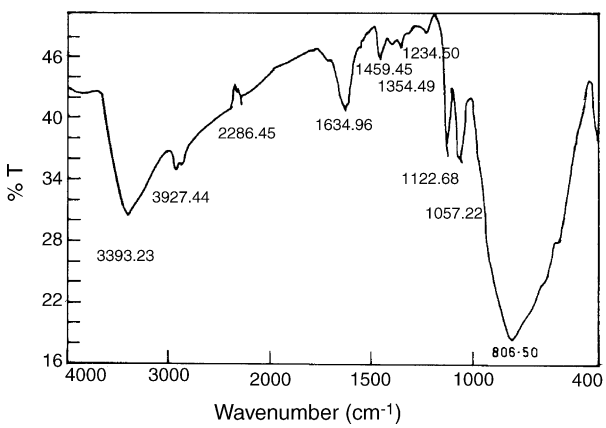

Fig. 2. FT-IR transmittance spectra of WO_3-precursor.

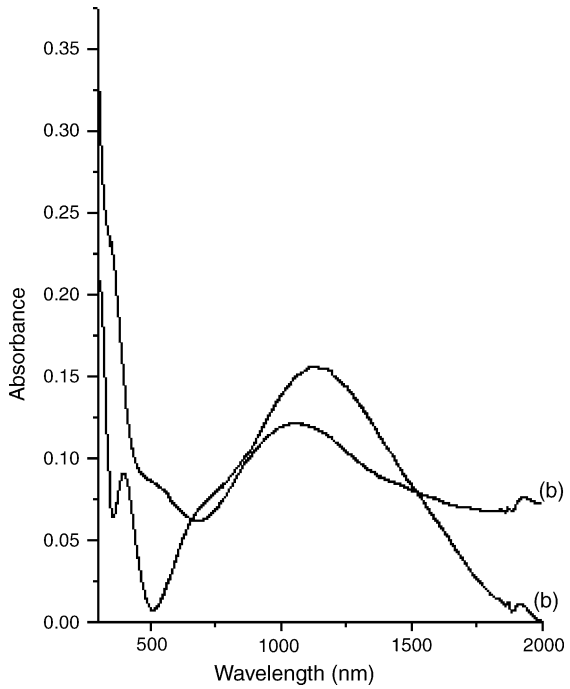

Fig. 3. Optical absorption spectrum of a thin film of the precursor on ITO glass electrodes obtained by spin coating: (a) WO_3, (b) WO_3:1% Ti.

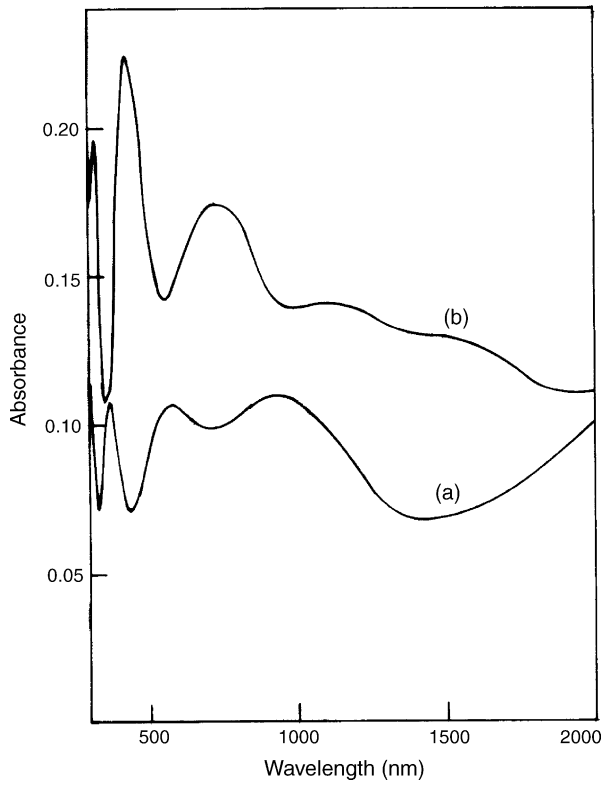

Fig. 4. Optical absorption spectrum of the samples annealed at 700 °C: (a) WO_3, (b) WO_3:1% Ti.

stretching frequency characteristics of WO_3 framework. The band at low energy side of the spectrum i.e. below 500 cm^{-1} is predominantly characterized by W–O asymmetric stretching frequency [19,20]. In the case of $WO_3 \cdot H_2O$ the peak was observed at 652 cm^{-1} and the peak at 800 cm^{-1} appeared as shoulders wherein in the precursor the peak was observed at 806 cm^{-1}. The other peaks also experience shifts in the frequency. The slight difference in the spectrum from that of the tungstic acid may be due to the non-stoichiometric nature of the precursor and the blue coloration is attributed to tungsten as an intervalent species, i.e. oxidation state less than W(VI) and greater than W(V). The FT-IR spectrum of WO_3 that was formed by annealing the precursor at 600 °C matches with the IR data of WO_3 in library (figure not shown). The band at 968 cm^{-1} in WO_3 corresponds to the W=O terminal vibrational mode stretching frequency [21]. The IR peaks due to H_2O molecule in the precursor is absent in annealed sample.

3.4. Optical spectra

Figs. 3 and 4 show the optical spectra of the precursor samples and the samples annealed at 700 °C, respectively. The precursor samples suspended in polyol and the samples heated at 700 °C were spin coated on a glass plate and the optical spectrum was recorded in the wavelength region 300–2000 nm.

The optical spectrum of WO_3 precursor shows a broad absorption spectrum around 1000 nm [22]. This is mainly due to the oxygen non-stoichiometry [23] and the formation of intervalent compound of W, i.e. W(VI) and W(V). In 1% Ti doped WO_3 there is a red shift of the fundamental absorption edge apart from the peak due to Ti. The red shift is mainly attributed to the weakening of W–O interaction and the decrease in the oxygen non-stoichiometry.

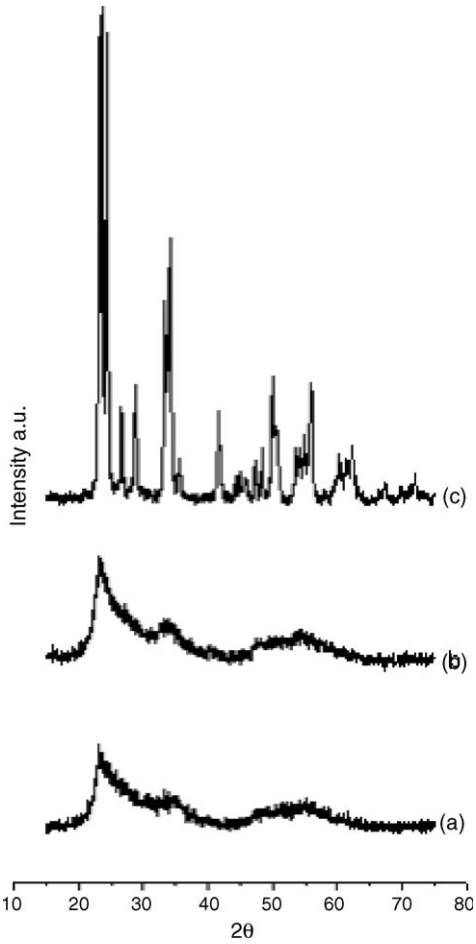

Fig. 5. XRD patterns of: (a) precursor of WO_3 as formed, (b) annealed at 300 °C, (c) annealed at 800 °C.

WO_3 annealed at 700 °C shows three absorption peaks due to intra band transition [24]. However, 1% and 10% Ti doped WO_3 shows red shift in the absorption peaks of WO_3 and the absorption around 400 nm is due to Ti centres [25]. The doping of Ti in WO_3 matrix decreases the bond length of W=O/O–W–O and as a result the optical band gap decreases. Hence the absorption takes place in the longer wavelength region leading to red shift.

3.5. XRD characterisation

The powder XRD pattern of the as formed precursor material is presented in Fig. 5a which exhibits three broad lines centred around 25°, 33° and 56°. This observation suggests that the material obtained by the hydrolysis of WCl_6 in polyol medium is poorly crystalline in nature. Fig. 5b and c show the XRD patterns observed for the samples of WO_3 obtained by annealing the precursor at 300 °C and 800 °C, respectively. It can be seen from the figure that there is no significant difference between the samples as formed and dried and the sample heated at 300 °C. This indicates that up to 300 °C the crystalline nature of the material did not change significantly. However, XRD pattern of the sample annealed at 400 °C (figure not shown) shows three major peaks between 20° and 25°. The peaks have high fullwidth at half maximum values (FWHM). The sample annealed at 800 °C showed sharp lines pattern. The pattern is compared with literature data reported by Depero et al. [26], Rao [27] and with the JCPDS data. The XRD pattern corresponds to the monoclinic phase where all the three major peaks are of comparable intensity and the other minor diffraction peaks also compare well with their simulated data. The same XRD pattern persists for the samples annealed at 600 °C and 700 °C as well (figures not shown) with the only difference being in the decrease in the peak height and increase in the

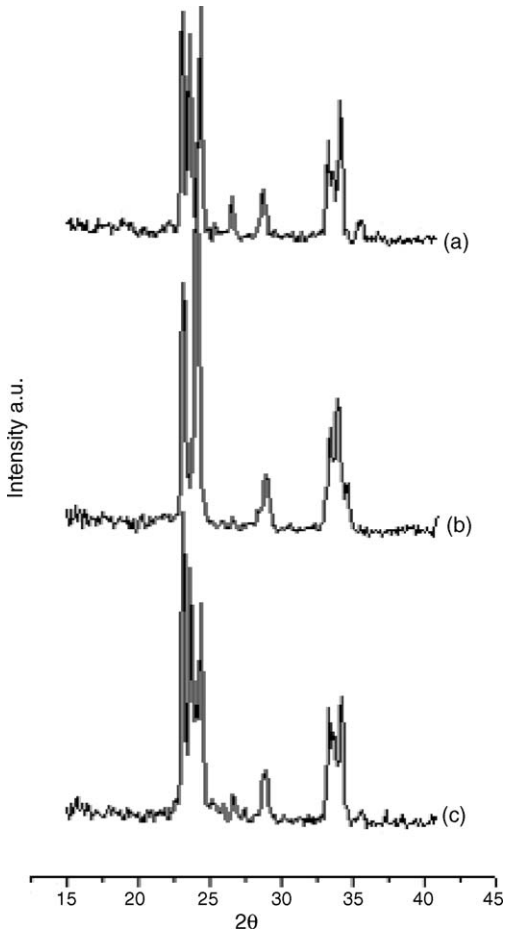

Fig. 6. XRD patterns of samples annealed at 700 °C: (a) WO_3, (b) WO_3:1% Ti, (c) WO_3:10% Ti.

FWHM values. This indicates that the crystallite size increases with the increase in annealing temperature. The average crystallite size D, was determined by Scherer's formula using the FWHM.

$$D = \frac{0.9\lambda}{B\cos\theta}$$

The crystallite sizes of the undoped WO_3 annealed at different temperatures ranging from 400 to 800 °C were calculated and found to vary from 10 to 30.8 nm.

Fig. 6a–c depict the XRD pattern of the WO_3:Ti (1% and 10%) annealed at 700 °C for 5 h along with that of undoped WO_3. The XRD patterns are significantly different from each other. The undoped WO_3, as already discussed exists in the monoclinic phase, whereas the Ti doped WO_3 samples (both 1% and 10%) are not monoclinic. Depero et al. [26] have simulated the XRD patterns for WO_3 for various crystal system, viz, triclinic, monoclinic, orthorhombic and tetragonal by introducing certain disorders. They have observed that in the case of WO_3, symmetries higher than monoclinic may result due to oxygen substoichiometry or doping with Ti, which has lower oxidation state than W. The diffraction pattern of WO_3:Ti(1%) closely resembles to tetragonal phase, wherein only two peaks are observed at 23.1562 and 24.068 (intensity 60:100) unlike the three peaks occurring at 23.07, 23.52 and 24.35 (intensity 100:90:100) in the case of monoclinic phase (JCPDS Files 5-0363 and 5-0388). However, increase in the concentration of Ti in the material, WO_3:Ti(10%) results in the decrease in the symmetry when compared to 1% Ti doped WO_3. Three major peaks are observed, but on comparing the data it could be deduced that the pattern corresponds to orthorhombic phase wherein the first peak is more intense unlike in the case of monoclinic phase.

From the XRD powder pattern we can clearly arrive at a conclusion that Ti can replace W from WO_3 that lead to corner sharing octahedra, resulting in the formation of tetragonal or orthorhombic phases. This is in accordance with

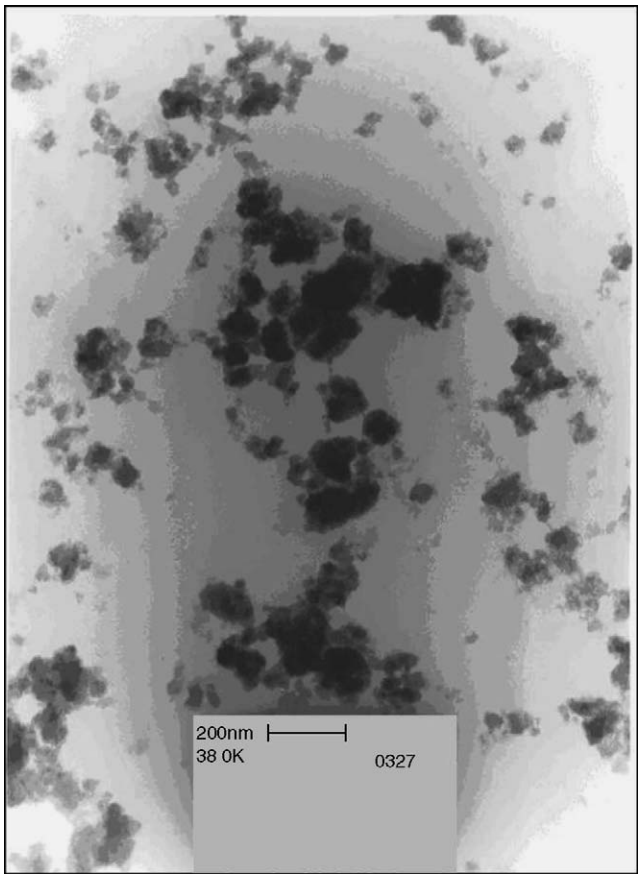

Fig. 7. TEM picture of WO_3 precursor formed in the polyol mediated synthesis.

the simulation studies of Depero et al. [26], wherein they have clearly showed that this type of corner sharing octahedra in WO_3 matrix leads to increase in the symmetry of the crystal lattice.

This is in contrast to the reports available in the recent literature. Komornicki et al. [15] have reported that when 1.15% Ti was doped in WO_3 a weak (1 1 0) reflex of rutile phase appeared ($2\theta = 27–28^\circ$). The WO_3 is also seen to have the monoclinic phase intact. They have concluded that stability limit of Ti in WO_3 is around 0.35 ± 0.05 mol%. It may be noted that both W(VI) and Ti(IV) have same ionic radii and hence Ti and W can occupy the same sites. The observations made by Komornicki et al. may probably be due to the inhomogenity in the preparative method that has been adopted. Alcoholysis of pure WCl_6 [9], yields WO_3 in orthorhombic phase at annealing temperature less than 550 °C and at temperatures over 700 °C it changes over to monoclinic phase.

3.6. SEM and TEM analysis

The TEM picture of the precursor material obtained by the hydrolysis of WCl_6 alone is depicted in Fig. 7. It can be seen from the figure that the particle size of precursor material is less than 100 nm. Similar trend has been observed for

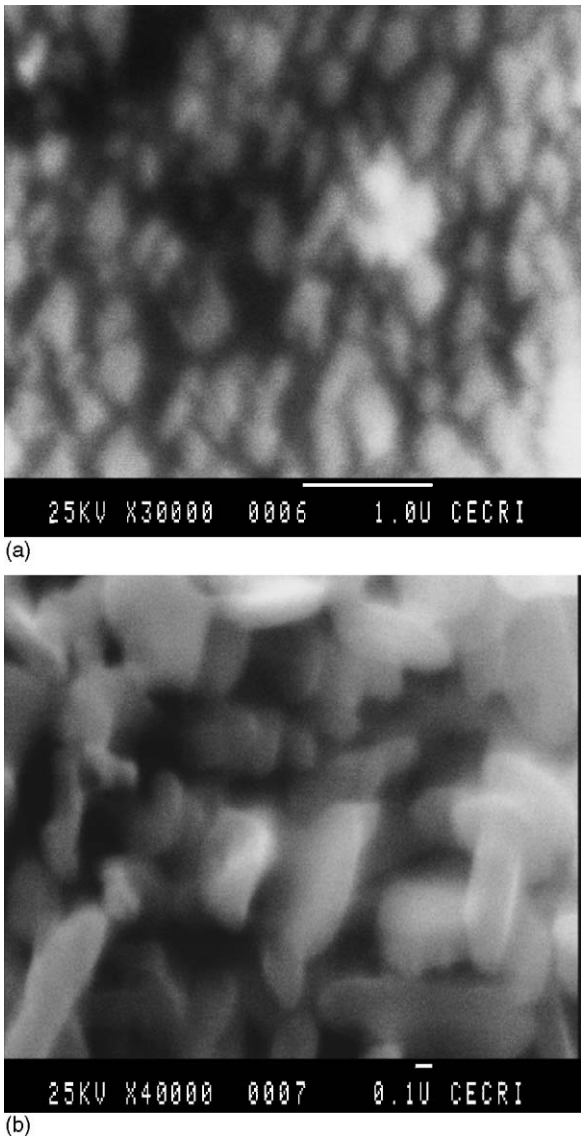

Fig. 8. SEM pictures of: (a) precursor of WO_3 formed in the polyol mediated synthesis, (b) WO_3 precursor annealed at 700 °C.

the titanium doped precursor materials as well. In Fig. 8a and b, the SEM pictures of the precursor material and the sample annealed at 700 °C are presented. A perusal of the pictures suggests that the nanometer sized precursor material grew into well-defined micron-sized crystals when annealed at 700 °C.

3.7. Electrochemical studies

The cyclic voltammetric studies of the precursor were carried using Pt electrodes in acidic media. The colloidal suspension of the precursor in polyol was coated on the Pt and heated at 200 °C for 2 h, leaving a blue coloured coating on the Pt electrode. This was used as working electrode and the cyclic votammogram (CV) was recorded in 0.1 M H_2SO_4 using a Pt wire counter electrode and Hg/Hg_2SO_4 (1.0 M H_2SO_4) as the reference electrode. The CV's of the precursor materials obtained using WCl_6 along with Ti doped ones are given in Fig. 9. It can be seen from Fig. 9a that the WO_3 precursor undergoes a redox process centred at −0.30 V wherein the reduction takes place at −0.420 V and the corresponding oxidation at −0.180 V [28]. During the recording of the CV it was noted that the film exhibits electrochromism. The blue colour disappears during anodic sweep and the colour is restored during the reduction cycle. The colouration can be attributed to the formation of F or F^+ centres in oxygen ion vacancies [29]. Repetitive cycling did not modify the voltammograms indicating the strong adherence of the precursor on Pt. This is attributed mainly to the electrochemical process involved in the reaction [29] represented by

$$WO_3{\cdot}H_2O + 2xH^+ \rightarrow xO^{\bullet\bullet}\,(\text{in}\,WO_3{\cdot}H_2O) + xH_2O$$

$$xO^{\bullet\bullet}\,(\text{in}\,WO_3{\cdot}H_2O) + 2xe^- \rightarrow WO_{3-x}{\cdot}H_2O$$

$xO^{\bullet\bullet}$ is the oxygen ion vacancies where the electrons are trapped, thereby resulting in the formation of W^V/W^{VI} in the matrix. The CV's were recorded for different scan rates like 10 mV/s, 25 mV/s, 50 mV/s, 75 mV/s and 100 mV/s and was noted that the peak current values varied linearly with the sweep rate indicating the redox process is surface bound.

Doping of Ti in WO_3 has significantly changed the voltammograms. In the case of 1% Ti doped WO_3 the CV shows (Fig. 9b) that the reversibility of the redox process has enhanced dramatically. The redox process occurs around the

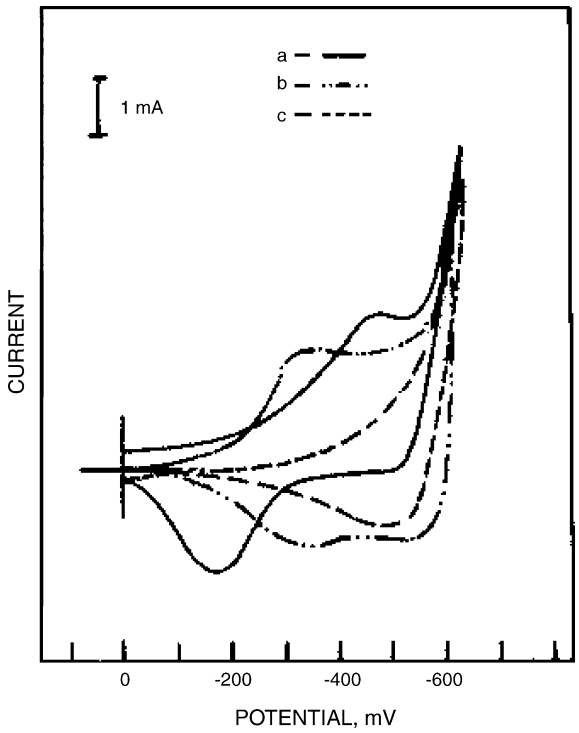

Fig. 9. Cyclic voltammograms recorded in 0.1 M H_2SO_4 for as formed: (a) WO_3, (b) WO_3:1% Ti, (c) WO_3:10% Ti coated on Pt electrode. Scan rate: 50 mV/s.

same potential window, viz., −0.33 V versus Hg/Hg_2SO_4(1.0 M H_2SO_4). Both the anodic and the cathodic peaks appear at −0.33 V, with a peak separation of zero mV. In the case of 10% Ti doped WO_3, the reduction process was found to be more difficult. The redox peaks have shifted to more negative potentials, the reduction peak was found to merge with the hydrogen evolution potential, wherein the anodic peak was broad and observed at around −0.5 V. These differences may essentially arise due to the difference in the structure of the oxide phase with variation in the doping level of Ti in the WO_3 matrix.

4. Conclusion

Polyol mediated synthesis for the preparation of WO_3 and WO_3:Ti was optimised. The particle size of the precursor was in the range of 100 nm. The precursor was annealed at a high temperature to yield WO_3 and WO_3:Ti. The precursor as well as the WO_3 and WO_3:Ti materials were characterised using optical absorption, FT-IR, TG/DTA, XRD and cyclic voltammetry. It was observed that doping of titanium in WO_3 lattice has changed the phase from monoclinic to tetragonal to orthorhombic depending on the percent of doping.

Acknowledgement

One of the authors P. Porkodi is thankful to Council of Scientific and Industrial Research, for the award of Research internship.

References

[1] T. Maruyama, S. Arai, J. Electrochem. Soc. 141 (4) (1994) 1021–1024.
[2] R. Sivakumar, A. Moses EzhilRaj, B. Subramanian, M. Jeyachandran, D.C. Trivedi, C. Sanjeeviraja, Mater. Res. Bull. 39 (2004) 1479–1480.
[3] Z. Wang, X. Hu, Electrochim. Acta 46 (2001) 1951–1956.
[4] J. Purans, A. Kuzmin, P. Parent, C. Laffon, Electrochim. Acta 46 (2001) 1973.
[5] C. Avellaneda, L.O.S. Bulhoes, Solid State Ionics 165 (2003) 117–121.
[6] L. Su, J. Fang, Z. Lu, Mater. Chem. Phys. 51 (1997) 85–87.
[7] D.-S. Lee, J.-W. Lim, S.-M. Lee, J.-S. Huh, D.-D. Lee, Sens. Actuators B 64 (2002) 31–36.
[8] E. Llobet, G. Molas, P. Molinas, J. Calderer, X. Vilanava, J. Brezmes, J.E. Sueiras, X. Correig, J. Electrochem. Soc. 149 (2) (2000) 776–779.
[9] V. Guidi, M. Blo, M.A. Butturi, M.C. Carotta, S. Galliera, A. Giberti, C. Malagu, G. Martinelli, M. Piga, M. Sacerdoti, B. Vendemiati, Sens. Actuators B 100 (1–2) (2004) 277–282.
[10] T. Hyodo, Y. Tominaga, T. Yamaguchi, A. Kawahara, H. Katsuki, Y. Shimizu, M. Egashira, Electrochemistry 71 (6) (2003) 481–484.
[11] D.-S. Lee, S.-D. Han, J.-S. Huh, D.-D. Lee, Sens. Actuators B 60 (1999) 57–63.
[12] J. Shieh, H.M. Feng, M.H. Hon, H.Y. Juang, Sens. Actuators B 86 (2002) 75–80.
[13] C. Lu, S.M. Kanan, C.P. Tripp, J. Mater. Chem. 12 (2002) 983–989.
[14] P.M.S. Monk, S.L. Chester, Electrochim. Acta 38 (11) (1993) 1521–1526.
[15] S. Komornicki, Mradecka, P. Sobas, Mater. Res. Bull. 39 (2004) 2007–2017.
[16] C. Feldmann, C. Metzmacher, J. Mater. Chem. 11 (2001) 2603–2606.
[17] C. Feldmann, Adv. Funct. Mater. 2 (13) (2003) 101–107.
[18] C. Feldmann, Scripta Mater. 44 (2001) 2193–2196.
[19] T. Nishide, F. Mizukami, Thin Solid Films 259 (1995) 212–217.
[20] M. Deepa, N. Sharma, P. Varshney, S.P. Varma, S.A. Agnihotry, J. Mater. Sci. 35 (2000) 5313–5318.
[21] M. Gotic, M. Ivanda, S. Popovic, S. Music, Mater. Sci. Eng. B 77 (2000) 193–201.
[22] S. Hashimoto, H. Matsuoka, J. Electrochem. Soc. 138 (8) (1991) 2403–2408.
[23] E. Ozkan, S.-H. Lee, C. Edwin Tracy, J. Roland Pitts, S.K. Deb, Sol. Energy Mater. Sol. Cells 79 (2003) 439–448.
[24] T. Kubo, Y. Nishikitani, J. Electrochem. Soc. 145 (5) (1998) 1729–1734.
[25] N.R. De tacconi, C.R. Chenthamarakshan, K.L. Wouters, F.M. MacDonnell, K. Rajeshwar, J. Electroanal. Chem. 566 (2004) 249–256.
[26] L.E. Depero, S. Groppelli, I. Natali-Sora, L. Sangaletti, G. Sberveglieri, E. Tondello, J. Solid State Chem. 121 (1996) 379–387.
[27] C.N.R. Rao, Pure Appl. Chem. 66 (9) (1994) 1765–1772.
[28] K.-I. Machida, M. Enyo, J. Electrochem. Soc. 137 (4) (1990) 1169–1175.
[29] C. Sunseri, F. Quarto, A. Paola, J. Appl. Electrochem. 10 (1980) 669–675.